

TMAL07 Report

UAV for Medical Payloads - MERAYU

Meet Akhil Kumar Agrawal, (meeag462)

Rakesh Nagaraja (rakna614)

Rohit Raja (rohra521)

Yuvarajendra Anjaneya Reddy, (yuvan983)

Academic supervisor: Alejandro Sobron

Examiner: David Lundström

Contents

1	Introduction	1
2	Subscale Design	2
2.1	Design Re-considerations	2
2.2	3-View	2
2.3	Specifications	4
2.4	List Estimation - Vortex Lattice Method	4
2.5	Components and Budget	6
2.6	Weights and Centre of Gravity	7
2.7	Structural Design	9
2.7.1	Fuselage	9
2.7.2	Wing	11
2.7.3	Empennage	13
3	Manufacturing	14
3.1	Production Files	14
3.2	Results	15
3.3	Risk Assessment	16
4	Flight Testing	17
5	Discussion and Conclusion	19

1 Introduction

Timely medical assistance in remote and rural areas in case of emergencies is a major concern around the world. In many cases, quick delivery of first aid and other basic medical supplies for self help aids in buying more time for professional medical attention. The most feasible mode of quick supply can be achieved by using drones as it can bypass all types of terrains and connectivity hurdles.

A concept UAV was generated for this purpose which can transport 4 kilograms of payload over a range of 120 kilometers at a cruising speed of 150 kmph. Upon arrival at the drop-off site, the UAV deploys the payload at a steady descent speed with the help of a parachute and the UAV returns back to the base for the next mission.

2 Subscale Design

The UAV has a simple, minimalist design with an unswept rectangular wing, conventional tail to operate effortlessly and complete the mission requirements. In order to simplify construction of the UAV, the same scale has been retained as the wing span lies below 2 meters and satisfies the dimensional restrictions.

2.1 Design Re-considerations

Before finalising the design of the UAV, a few other options were considered to evaluate the feasibility and efficiency. The changes considered were:

- 1) An Uncovered Tail arm with exposed boom:

The intention behind this consideration was to minimize weight. But it would create more pressure drag from the wake region as there was a sharp end to the fuselage.

- 2) V-Tail:

If option 1 was considered, then the vertical tail efficiency would be greatly minimised because of the wake region. Hence, a V-Tail configuration was evaluated to avoid interference with the vertical tail.

- 3) T-Tail:

A common problem with high wing aircrafts is the elevator shadowing at high AoA. Hence a T-Tail configuration was also considered.

After a Strength/Weakness analysis, the original design was retained since it had more advantages. A slight fuselage resizing was performed as it was oversized and had a lot of empty space. The control surfaces were also resized as the original design had undersized control surfaces. Additionally, flaps were removed from the original design as the wing can produce enough lift force at the given flying conditions.

2.2 3-View

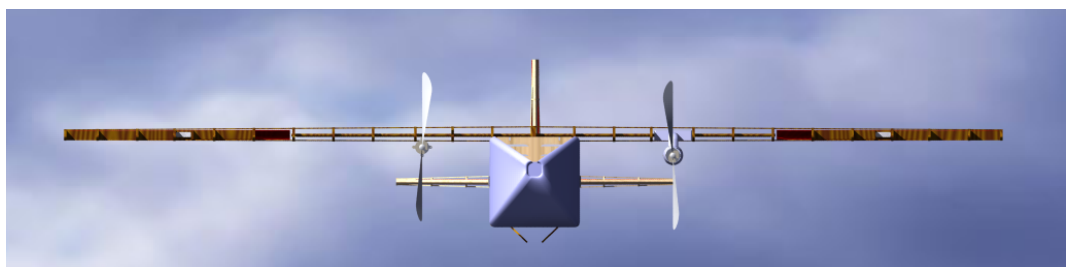


Figure 1: Front View of the final CATIA Model

Figures. 1, 2, 3, 4 shows the different views of the aircraft.

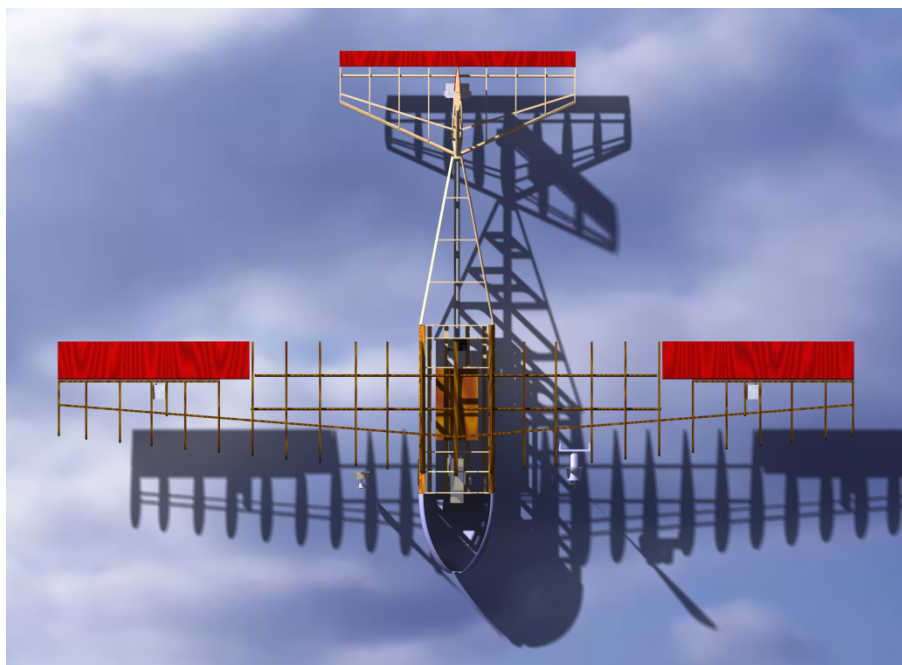


Figure 2: Top View of the final CATIA Model

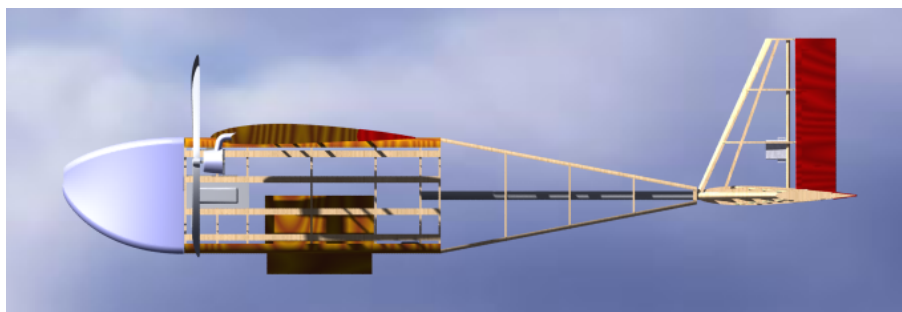


Figure 3: Side View of the final CATIA Model

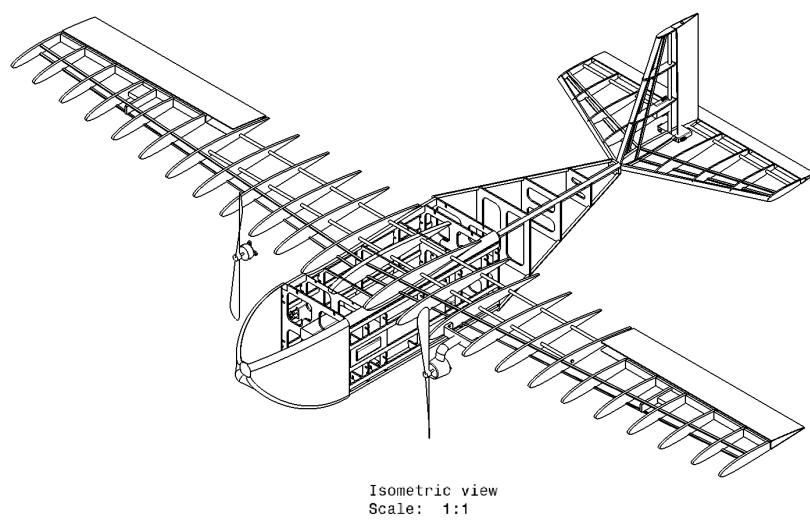


Figure 4: Isometric Drawing of the final CATIA Model

2.3 Specifications

The full specifications of the UAV is mentioned in Table. 3.

Specifications	Value
Wing Span	1.82 m
Length	1.234 m
Wing AR	7
Wing Root Chord	0.318 m
Horizontal Tail Span	0.56 m
Horizontal Tail AR	3
Vertical Tail	0.23 m
Vertical Tail AR	1.5
Mean Aerodynamic Chord	0.273 m
Centre of Gravity	30 % of MAC: 0.322 m

Table 1: MERAYU Specifications

2.4 List Estimation - Vortex Lattice Method

An initial lift estimation is carried out to determine the lift distribution across the main wing and the empennage using Tornado Vortex Lattice Method toolkit. The bending moments across the wing is also estimated by this method. The Tornado tool divides the surface of the wing into panels and estimates the lift and bending moment over each panel.

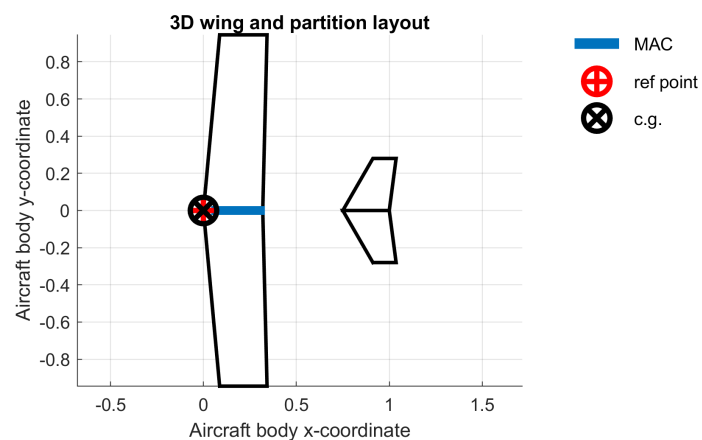


Figure 5: 3D Partition Layout

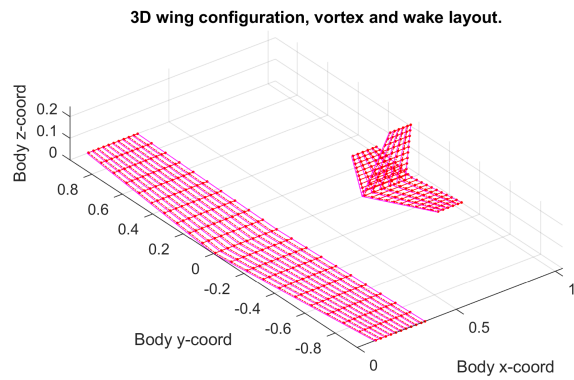


Figure 6: 3D Wing Configuration

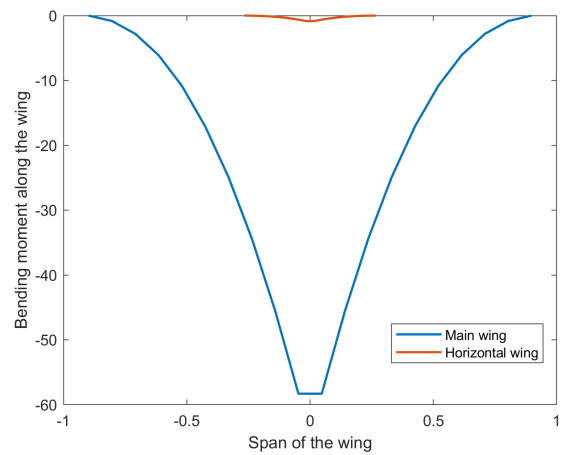


Figure 7: Bending moment Distribution

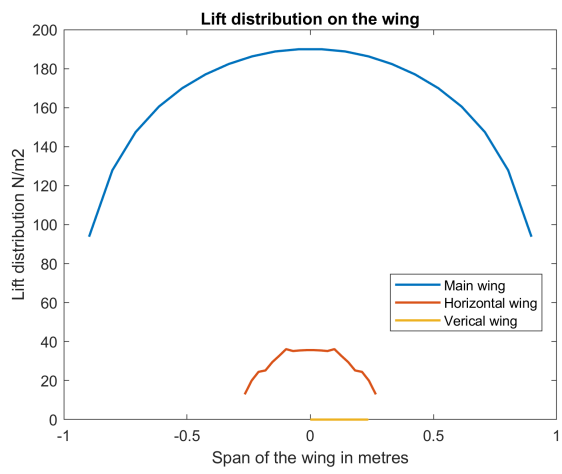


Figure 8: Lift Distribution

2.5 Components and Budget

A detailed breakdown of the cost of component is given in Table. 2. The budget was capped at 3000 SEK, but since the UAV consists of two motors, the cost of electronics (Motor, ESC, Battery) doubled and the overall cost unfortunately crossed the limit and reached 3372 SEK.

Description	Quantity	Price - Each (SEK)	Price - Total (SEK)
Motor for Twin Engine	2	219	438
Propeller	2	35	70
ESC 30A	2	150	300
Battery 2200 mAh	2	250	500
RC Receiver	1	370	370
Regular Servo	4	80	320
Thin Servo	1	95	95
Servo Extension Cables	4	10	40
Orange Covering Film	4	20	80
Black Covering Film	4	20	80
Balsa sheet 3x100x1000	9	22	198
Balsa sheet 5x100x1000	10	28	280
Pine Wood 3x3	3	5	15
Pine Wood 2x5	4	5	20
Liteply 3x200x1000	3	65	195
Carbon tube (ud) 10x1000mm	2	70	140
Carbon tube (ud) 12x1000mm	1	90	90
Metal Pushrod	5	7	35
Metal Snap Link	5	5	25
Rudder Horn	5	9	45
Plastic Hinge	12	1	12
M5x40 Nylon bolt	1	24	24
		Total	3372

Table 2: Bill of Materials

2.6 Weights and Centre of Gravity

Component	Weight (Grams)
Fuselage:	
Nose	177
Fuselage Ribs	234
Tail Boom	46
Skin	150
Empennage	
Horizontal Tail	46
Elevator	10
Vertical Tail	15
Rudder	7
Wing	
Wing Ribs	149
Skin	103
Ailerons x2	74
3D Printed Components	
Boom Support x2	58
Tail Support Cap	121
Pylon Plates x2	28
Pylons x4	28
Nacelles x2	30
ESC Cooling Flush inlets x2	16
Electronics	
Servo x5	115
ESC x2	56
Extension Cables	100
Other	
Motors x2	24
Propellers x2	32
Payload	200
Total	2317

Table 3: Component wise Weight Breakdown

The Centre of gravity is located at 30 % of Mean Aerodynamic chord and 0.322 m from the nose in x-direction. It is important for the CoG to lie at around 25 percentage of the Mean Aerodynamic Chord as maximum lift is generated at this region. As the CoG moves away from the Mean Aerodynamic chord, a moment is created between them and the pitch will be affected as a result.

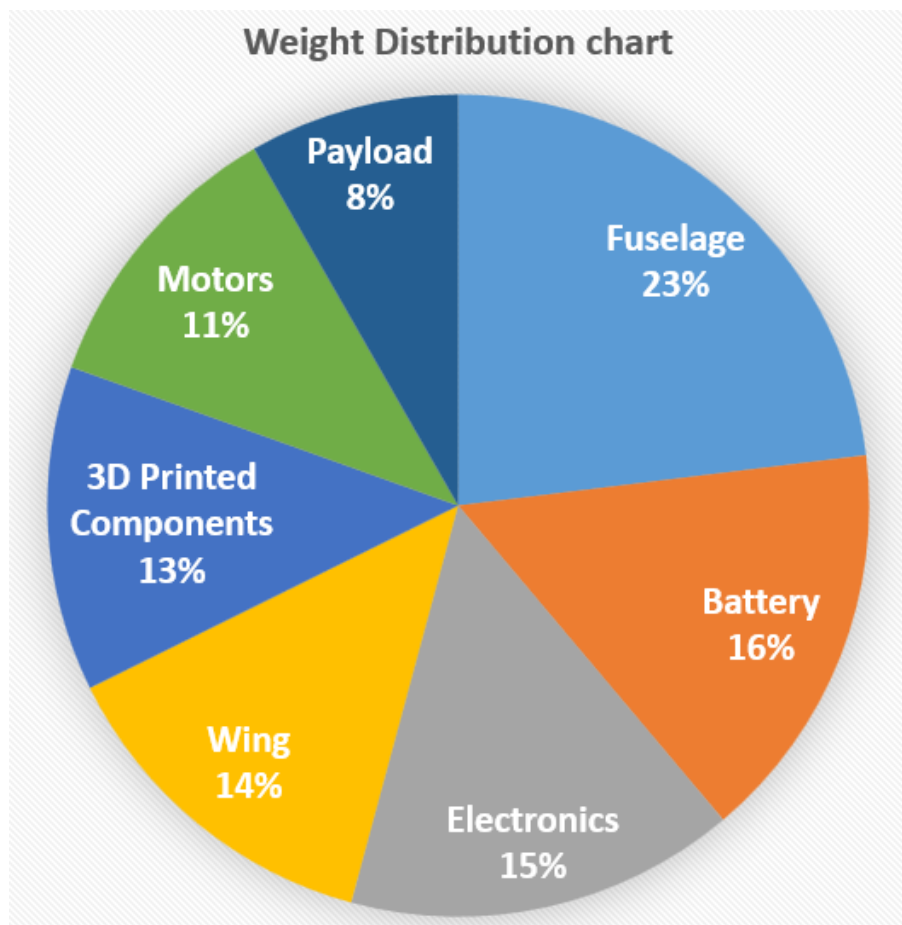


Figure 9: Weight Distribution chart for the UAV

2.7 Structural Design

2.7.1 Fuselage

The ideal shape of a fuselage would be cylindrical in shape considering the cabin pressurisation exerts even loads on the fuselage and stress concentration is avoided. Also, from an Aerodynamic perspective, it produces lesser drag. But a cylindrical fuselage usually leads to unused space inside. Since, our cabin will not pressurised and the UAV is used for low speed applications, we decided to select a rectangular fuselage with rounded edges. This offers more volume inside the fuselage and is also easy to manufacture with good wing mounting options.

The fuselage is divided into two sections during the design phase: Main fuselage section and the tail arm section. The main fuselage section is designed with multiple frames positioned in parallel. These frames are made out of liteply as they are the primary load bearing members. These frames consists of jigsaw slots around the edges where the Longerons are placed to keep the frames in place and offer structural support and 4 stringers made out of Balsa wood are glued at the corners to provide the curved shape. On the top surface, the Longerons are slightly sanded to take the shape of the wing's chord as seen in Fig. 10.

The tail arm section of the fuselage does not offer any structural support, but is design purely for Aerodynamic merits. This section helps to keep the flow attached and thereby reducing pressure drag. The tail arm section consists of 3 frames placed in parallel with 4 stringers at the corners of the frames. The loads in this section are taken up by the boom which runs from the main section of the fuselage till the empennage. The boom is coupled with the last two frames of the main section of the fuselage and transfers all the loads from the empennage to these two frames. As a reinforcement, a 3D printed Boom support fixture as seen in Fig. 11 are glued and screwed on these frames to prevent splintering of the frames and to transfer the loads more evenly.

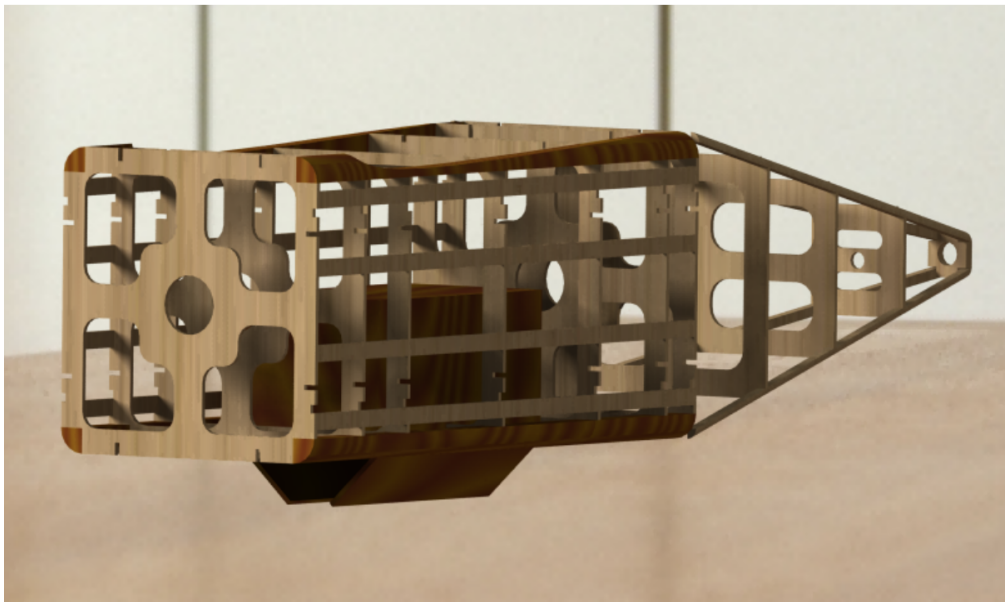


Figure 10: Isometric view of the Fuselage



Figure 11: Boom support fixture

Since, a detachable wing was a design requirement, two plates with M5 bolting holes were designed which were made of pine wood. One plate was attached to the fuselage and the other plate was attached to the wing. The wing could be attached to the fuselage by using four M5 bolts to keep them securely intact.

Additionally, the Fuselage houses all main electronics like: Receiver, ESCs and Batteries. As the ESCs become hot during flight due to electrical resistance, two 3D printed flush air intakes are mounted on either side of the fuselage to ensure cooling airflow over the ESCs to avoid heat damage.

Lastly, a payload drop door is designed at the bottom of the fuselage in order to drop the payload as per the mission requirements. The drop doors open outwards which is controlled by a servo which is mounted inside the fuselage. All the components inside can be easily accessed by opening the payload drop door.

The nose section of the aircraft is 3D printed in four different phases due to the dimensional constraints of the 3D printer. All the four parts are then glued together with the help of epoxy. The first section of the nose is equipped with an L clamp which is used to attach the nose to the fuselage as seen in Fig. 12. This interface is managed with the help of velcro strips.



Figure 12: Nose attached to the Fuselage

2.7.2 Wing

MERAYU employs a conventional rectangular wing with a wing span of 1.82 m and an Aspect ratio of 7. The root chord of the wing is 318 mm. Since the wingspan is quite large, the wing is built in two parts: left half and right half to simplify construction. One half of the wing consists of 13 ribs placed equidistant in parallel. The ribs are made out of 3mm Balsa wood as seen in Fig. 13. Similar to the fuselage frames, the wing ribs also have jigsaw slots and cavities for reducing weight as seen in Fig. 14.

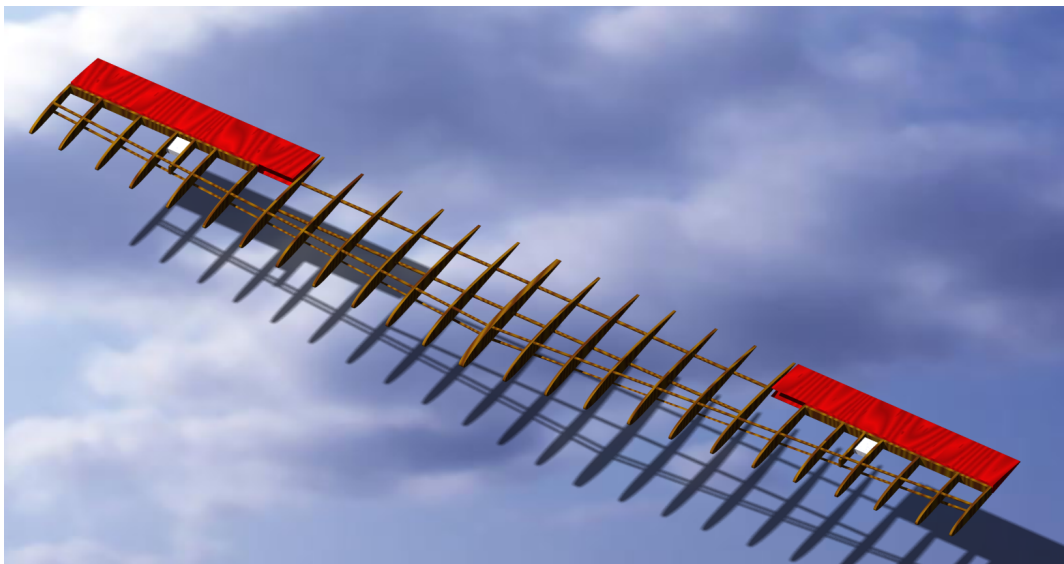


Figure 13: Isometric view of the Wing

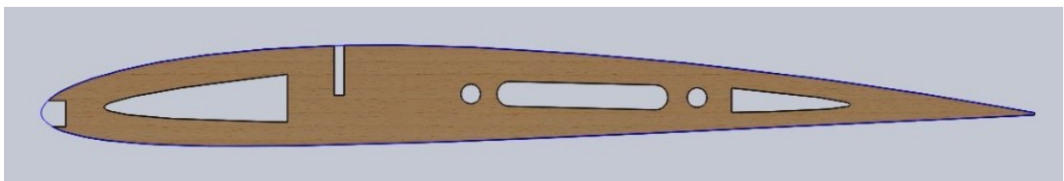


Figure 14: Profile of the wing rib

Apart from producing lift force, other important design considerations for the wing are: Bending loads, Torsional loads, shear loads. In order to design a wing which can withstand all the mentioned loads, suitable reinforcements have to be provided to the ribs. For this, we employ a 3 stage reinforcement strategy.

The primary load bearing member is called the main spar which is approximately in the centre of the Root chord. The main spar is a unidirectional carbon tube with a diameter of 10 mm. This spar runs from Aileron to Aileron covering approximately half of the wing span 1m. The intention behind the main spar is to absorb bending loads especially in the region where the left half and right half of the wing is joined. The second reinforcement is called the sub-spar which is located near the trailing edge. The sub-spar is unidirectional carbon tube with a diameter of 6 mm. Unlike the main spar, the sub-spar is broken down into two halves meant for each half of the wing which runs from the root chord to the tip chord. The sub-spar helps in

absorbing torsional loads.

The last reinforcement is a rectangular wooden spar made out of 3mm lite-ply which is located near the leading edge of the chord. This is also divided into two halves, one for each half of the wing. Unlike the carbon tubes, the wooden spar is parallel to the leading edge and hence remains equidistant from the leading edge throughout the wing. This spar is introduced to provide additional torsional rigidity. All three spars combined provide good shear loading capacity and also helps to withstand impact loads and whiplash effects.

As explained earlier, the wing is detachable, hence the mounting plates are attached near the root chord in alignment to the mounting plate present in the fuselage. As a backup, a 3D printed wing clamp as seen in Fig. 15 is also present on the main spar which can be clipped on to the fuselage frame for extra support.



Figure 15: Wing Clamp

Since we have a wing mounted engine configuration, the powerplant assembly needs to be integrated with the wing. The Powerplant assembly is made of 3 parts which are 3D printed. A pylon plate is mounted between two wing ribs. The arms of the pylon plate are extended till the wooden spar to provide more surface area for gluing and to transmit the thrust loads to the wooden spar. Two pylons are then added to the pylon plate with glue and screws. The pylon consists of a U-Bend which clamps the pylon plate from behind which helps in transferring the thrust loads to the pylon plate more efficiently. Finally, the nacelle is attached to the pylons with the help of screws and cyanoacrylate glue to complete the powerplant assembly as seen in Fig.18. The motor is then screwed to the rear surface of the nacelle.

In order to attach the ailerons to the wing, a second layer of Balsa is added behind the trailing edge in order to provide more surface area for the plastic hinges to be seated. Three hinges are used for each Aileron which is to be secured by pouring a drop of cyanoacrelate glue on the hinge. The aileron is actuated by a servo which is placed inside the wing. The Aileron is connected to the servo with the help of a metal push rod where the push rod remains outside the wing. The servo is then connected to the receiver with the help of extension cables which pass through the cavities in the wing and into the fuselage. The Ailerons have a total actuation range of 45 degrees.

The leading edge and trailing edge of the wing are covered with 1.5mm balsa sheet in order to provide enough surface area for the plastic film to adhere and also to avoid depressions of heat shrunk plastic film between two ribs.

2.7.3 Empennage

The last structural component of the aircraft is the empennage which consists of a Horizontal Tail, Elevator, Vertical Tail and Rudder. The empennage reinforcements are similar to the wing reinforcements. But the HT and VT consists of only one main spar which is a 6 mm carbon tube and a rectangular 3mm lite-ply spar which is parallel to the leading edge. The purpose of usage of spars is similar to the wing. Elevator and rudder attachment is also similar to the wing.

The HT and VT are integrated by mounting them on the 3D printed Tail support cap which consists of profiles of the root chords of HT and VT. The root chords are then glued and screwed to the Tail support cap as seen in Fig. 16 and Fig. 19. For additional stability, the main spars of HT and VT are made to pass through the tail support cap.

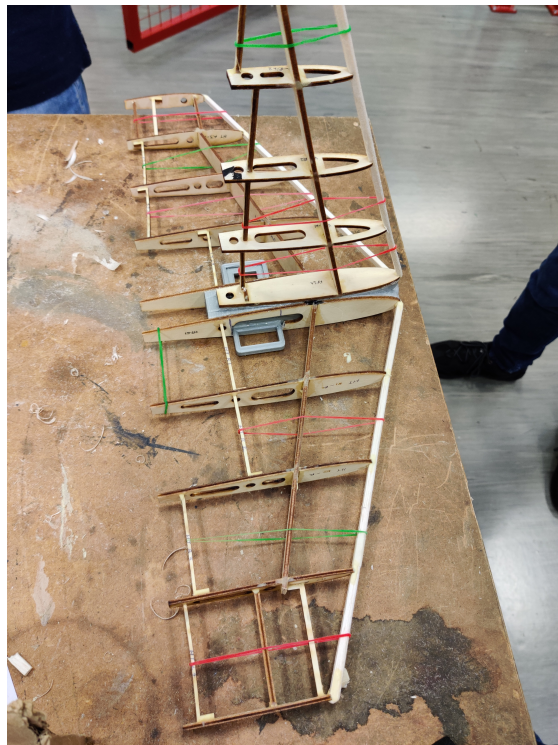


Figure 16: Skeleton of the Empennage

The elevator and rudder is attached to the HT and VT similar to the wing, using plastic hinges. The servos are mounted on either sides of the Vertical Tail. One servo is connected to the rudder and the other servo is connected to the elevator. The push rod connecting the elevator had to be bent away from the rudder as it was obstructing the actuation of the rudder.

The Empennage assembly is then connected to the boom and it is glued together using epoxy.

3 Manufacturing

3.1 Production Files

As seen in Fig. 17, multiple files were drafted for Laser cutting which consisted of all the ribs in the Wing, Ailerons, Horizontal Tail, Elevator, Vertical Tail and Rudder, and also for all the frames in the fuselage. The ribs were carefully placed close to each other to minimise wastage and also to expedite the cutting process. A common protocol followed for laser cutting is to mark all the primary cuts in Red colours, all the secondary cuts in Green colour and lastly all the Engravings in Blue Colour. Laser cutting can be used for cutting Balsa or Lite-ply sheets upto 5mm thickness.

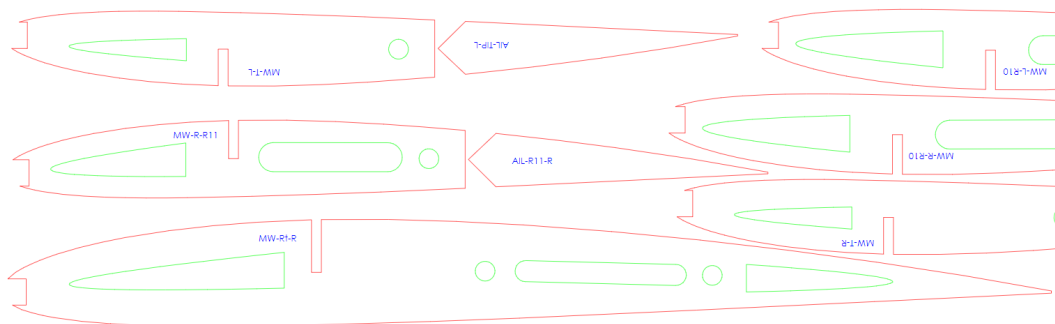


Figure 17: Production Files for Laser Cutting

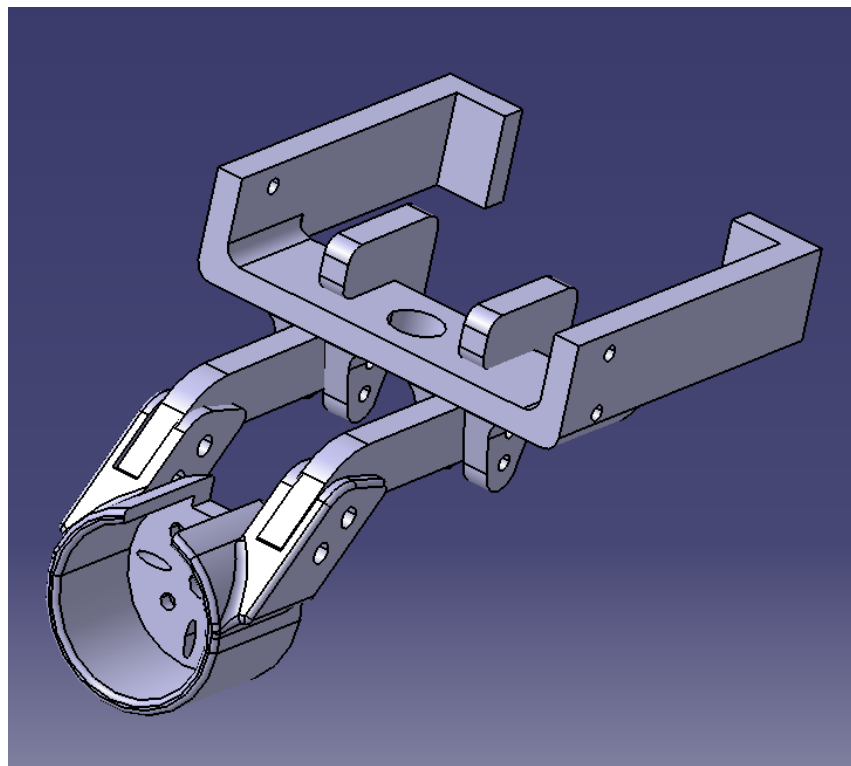


Figure 18: Isometric view of Power Plant Assembly

The power plant assembly as seen in Fig. 18 is printed using PLA material in 3 different stages and later assembled together. This makes 3D printing easier and avoids the use of excessive support material. From the experience of printing complicated geometries, it is advised to use PLA support instead of PVA support as it is faster, more stable and less chances of failures. If the support needed is too tall, then there is a very high probability of PVA support failure. But PLA support cannot be used for internal holes as it would be difficult to remove them.



Figure 19: Isometric view of Tail Support Cap

Fig. 19 shows the Isometric view of the Tail Support cap on which the HT and VT are mounted. The assembly is later inserted into the boom to be integrated with the fuselage.

3.2 Results

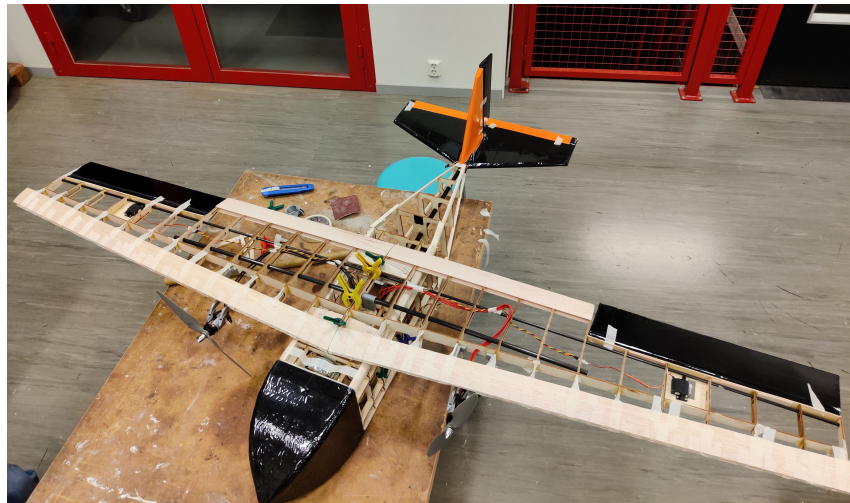


Figure 20: UAV at the final stages of production

In Fig. 20, the UAV can be seen fully assembled but without the plastic film.

Placements of all components like electronics, spars, cables etc. can be easily seen here.

When compared with the predictions, we observed a couple of noticeable deviations. Most of the weights estimated from CATIA were accurate. A physical CoG estimation was carried out when the aircraft was ready, by using a roller under the aircraft and sliding it over the roller to determine the CoG in reality. It turned out that the CoG had shifted further down from 30 %. It was advised to keep the CoG at 25 % for a stable flight. Hence, we had to introduce Ballasts in the nose which weighed approximately 400 g. This was still not sufficient to get the CoG to 25% of MAC. Hence, instead of adding more ballasts, we decided to mount a video camera on the nose which weighed 170 grams. This got the CoG to exactly 25 % of the MAC at 0.308 m from the nose in x-direction.

The added weights of 400 g of ballast, 170 g of video camera and the extension cables turned out to be approximately 200 g which was twice the initial estimation of 100 g. This led to a total increase of 670 g from the original estimation.

Hence, our Final aircraft weight turned out to be 2987 grams which was almost 3 kgs.

3.3 Risk Assessment

Risk Description	Severity: 1 - Low, flight not compromised 2 - High, Flight Compromised 3 - Catastrophic	Probability: 1- Low 2- Medium 3- High	Mitigation Action(s)
Stall speed not achieved during takeoff	2	1	Powerful hand launch required
Servo Failure	2	1	Control with remaining servos
Nacelle Assembly Fails	3	2	Land Immediately with motors switched off
Structural Failure	3	1	Reinforce Suspected weak members
Push rod breaks	2	1	Control with remaining control surfaces and land soon
Payload not deployed	1	3	Move UAV rapidly and try to force it out
Propeller ground strike during landing	1	1	Try to land with the wings parallel to the ground
Impact Damage upon landing	1	2	Try to land smoothly
Electronics Failure	2	1	Do not overload any component
Centre of Gravity variation	2	1	Use trim tabs to counter-act pitch or roll

Figure 21: Pre-Flight risk assessment

An extensive pre-flight risk investigation is performed to evaluate the probabilities of failure of different components and it's consequences as seen in Fig. 21.

4 Flight Testing

The first flight test day was an unfortunate day as the left motor failed due to nacelle interference. Once, the problem was fixed, the second flight test day was successful. A steady take off was observed and a healthy climb rate was achieved. The effectiveness of the control surfaces was first checked, which turned out to be good. Following the mission profile, the UAV tried to deploy the payload by opening the bay doors. But it was not deployed because the size of the payload and the size of the bay door was very close and the payload could've got dislocated during climb or maneuvering.

Further, the UAV was pushed to it's limits to check it's maneuvering capabilities. An inverted flyby, barrel roll, vertical climb, stall recovery, high altitude cruise etc. were all tested and the UAV performed exceptionally well. The inverted flyby was done for a very long time, this could be achieved due to a near-symmetric airfoil used. During final approach, the left nacelle failed because the space had interfered with the nacelle wall and generated so much heat which was enough to melt the plastic and dislodge the screws. Luckily, the aircraft was flying well above the stall speed and it was able to glide to a safe landing. The burnout caused significant damage to the motor as there was melted plastic residue on the motor shaft. Upon hard landing, one of the fuselage frames had cracked at the bottom surface, but did not cause any problems to the structural integrity.



Figure 22: Fly-By

After the flight test, the pilot reported a nose heavy aircraft, which might have been due to excess ballast. This problem was resolved by removing 50 grams of

ballast from the nose. Also, the pilot reported a reduced efficiency of the rudder. This could be due to the turbulence generated by the Video camera mounted on the nose which choked the rudder. The elevator area was slightly undersized and it could have been larger to provide better pitch controls.



Figure 23: Inverted Fly-By



Figure 24: Vertical Climb

5 Discussion and Conclusion

The intentions of this course have been achieved. We got incredible exposure towards aircraft design and manufacturing. Several challenges during the design phase and manufacturing phase came to light and was resolved with the help of research and guidance. However, there is plenty of room for improvements. The main improvement which comes to mind is the reliability and durability. Many components were designed with a low Factor of safety. This can be improved by providing better reinforcements. Additionally, the wing mounted nacelles offer various design choices which can be further evaluated and designed for better reliability. The flight mechanics can be further investigated to improve the controllability of the aircraft. The payload housing area can be better which does not allow the payload to dislocate from its position.

Overall, it can be considered as a success as it completed the mission profile and was able to perform many maneuvers.



Figure 25: On-board camera footage during vertical climb